Environmental Processes (2021) 8:843–867
https://doi.org/10.1007/s40710-020-00493-w

ORIGINAL ARTICLE

Effect of Nanosized TiO_2 on Redox Properties in Fenugreek (*Trigonella foenum graecum* L.) during Germination

Takwa Missaoui [1,2] · Moêz Smiri [1,3] · Hajer Chemingui [1] · Amor Hafiane [1]

Received: 22 July 2020 / Accepted: 23 December 2020 /Published online: 11 March 2021

Abstract
The goal of the present work was to identify the most important physiological and biological effects of titanium dioxide nanoparticles (TiO_2 NPs) at a size of 83 ± 15 nm on plant parts. This was done by studying TiO_2 physical and chemical properties through X-ray diffraction, scanning electron microscopy, Fourier transform infrared spectroscopy (FTIR), and Dynamic Light Scattering, and how TiO_2 NPs move in plant organs and in the most important plant cells. Fenugreek (*Trigonella foenum graecum* L.) exposed to 100 mg L^{-1} of TiO_2 NPs increased chlorophyll-a and -b and polyphenol contents, and decreased flavonoid level of leaves. Nano-stressed leaves and stems, therefore, displayed substantially increased catalase and ascorbate peroxidase activities. On the contrary, guaiacol peroxidase activities in the leaves and stems exposed to TiO_2 NPs were significantly reduced. The result after 16 days of exposure to metal oxide was a substantial increase in the levels of nicotinamide adenine dinucleotide oxidase (NADH) in the leaves but a decrease in lipid peroxidation in the stems. The effects caused by exposure to NPs are regulated by specific isoforms of each compartment and each organ. TiO_2 NPs were accumulated in the cell wall, resulting in the closure of plant cell pores that finished with the suspension of functions of the most important organelles targets such as mitochondria. We suggest that nanoparticles with size higher than 83 nm are transported via apoplastic pathway. Based on the correlations between mitochondria and cell apoptosis, accumulation of TiO_2 in the cell wall causes lipid peroxidation and cell death. Metabolites changes in plants exposed to nano stressors have been determined by FTIR microspectroscopy. Environmental effect and risk of nanomaterial contamination have been studied after analyzing antioxidant enzymes. The role of oxidative stress markers in plant responses was well established.

Keywords Anthocyanins · Nanotoxicity · Oxidative stress · Photosynthesis · Titanium dioxide · *Trigonella foenum graecum* L

✉ Moêz Smiri
almoez@su.edu.sa; smirimoez@yahoo.fr

Extended author information available on the last page of the article

1 Introduction

A significant area of study in modern science is nanotechnology. The use of nanomaterials in various fields is of great benefit because of their properties and nanoparticle activity (Satalkar et al. 2016). According to the literature, there are five groups of nanomaterials: carbon nanoparticles (NPs), metal oxides, quantum dots, zero value metals and nanopolymers (Hund-Rinke et al. 2020).

Nanoparticles can be present in combined forms in the environment. They can undergo a large range of physical, chemical, and biological modifications (adsorption, aggregation, agglomeration, or redox reaction). Also, many other parameters, like pH, the presence of organic matter, salinity, and the presence of microorganisms in the soil, can influence the reactivity, toxicity, and mobility of nanoparticles in the environment. Besides, the complexity of environmental matrices and their low concentrations in the environment become their identification difficult. Consequently, adapting current technologies and designing new technologies to recognize, measure and classify these nanoparticles in ecosystems is a challenging work (Naghdi et al. 2017; Bundschuh et al. 2018).

Plants are located at the interface between the three ecosystems (water-soil-air). Indeed, they are anchored in the soil, feed on water (soil solution) and exchange with air. Plants are also at the base of the food chain going to humans. This link is, therefore, fundamental to the study of the impact of nanomaterials on the environment. Plants are the first to be exposed to pollutants, including nanoparticles. Also, as previously stated plants have a crucial ecological role in ecosystems and are of particular interest in ecotoxicology studies as sentinels (Planchuelo et al. 2019).

Due to its interesting general properties, titanium dioxide (TiO_2) has been intensively researched in a wide variety of fields that influence quality of life, including catalysis and photocatalysis, as antibacterial agent, and in construction as nano-paint (self-cleaning). The interesting physical and chemical properties of TiO_2 depend on the crystal phase, size and shape of particles. It also exhibits electrical, optical and morphological characteristics that make TiO_2 preferred in environmental applications (Haider et al. 2019). For these reasons, it allows its application in the agricultural sector. TiO_2 NPs with improved performance can be used for pesticide degradation, plant germination and growth, management of crop diseases, water purification and identification of pesticide residues (Shang et al. 2020; Nile et al. 2020). Numerous articles have emphasized the beneficial effect of TiO_2 NPs on plant growth. Chutipaijit and Sutjaritvorakul (2020) investigated the callus formation, plant metabolites and antioxidant activity of callus and callus extract from indica rice cv. Pathumthani. When treated with TiO_2 NPs, the high levels of total phenolic compounds, flavonoids and antioxidant activity of callus extract gave a promising sign that a functional supplementary product from agriculture, food and cosmetic applications could be improved. Song et al. (2020) found that appropriate doses of TiO_2 NPs have the potential to increase plant production by increasing plant photosynthetic rate without inducing excessive stress or toxicity of cucumber, but negative effects can be observed when NPs were used: Wu et al. (2017) observed that TiO_2 NPs decreased the biomass and the content of carbohydrate, while the contents of proteins, lipids, and antioxidants defense system in rice increased. Additionally, the reactive oxygen species (ROS) induced by TiO_2 NPs can break the cell membrane of plant, decrease the biomass, affect the enzymatic activities of the antioxidant defense system, decrease photosynthesis, and damage deoxyribonucleic acid (Xia et al. 2015; Deng et al. 2017; Middepogu et al. 2018). Thus, it is essential to understand the importance of TiO_2 NPs on plant species metabolic processes, and perhaps even the aims and mechanisms behind their potential future phytotoxicity.

The leaves surface area, the length and the weight of the stem and roots are morphological markers of plant development. Ghoto et al. (2020) assert that plant growth and biomass of maize were not affected by TiO_2 NPs of 30 nm (1000 mg/L). Missaoui et al. (2017) studied the

effects of nanosized titanium dioxide on the photosynthetic metabolism of fenugreek (*Trigonella foenum-graecum* L.) and reported that there were no important impacts on the development of seedlings and stem biomass, but a reduction in the leaf's fresh weight after treating with 100 mg L^{-1} TiO_2 NPs of less than 20 nm size.

One of the assumptions stressed for the toxicity of TiO_2 NPs in aerobic organisms were associated with oxidative stress as an increased effect of ROS and redox imbalance in status. Metabolic processes in aerobic organisms, like plants, generate ROS molecules as intermediate products of the reduction of oxygen (O_2) to water (Janků et al. 2019). Plants continually produce ROS in organelles such as chloroplasts, mitochondria, peroxisomes, the endoplasmic reticulum, and plasma membranes (Janků et al. 2019; Verma et al. 2019). Similarly, ROS molecules do not accumulate because they are continually removed by the non-enzymatic or enzymatic defense complex system. The components of the system are variable depending on their catalytic activity, their molecular weight, the compartment in which they act and their degree of defense or mechanism of action. There are several biotic and abiotic factors that alter the equilibrium between production and removal of ROS (Verma et al. 2019). It could be explained in part by TiO_2 NPs, even without ultraviolet (UV) radiation, to produce free radicals. On the other hand, it is still unclear how the direct interaction of these NPs with plant biological molecules and tissues eventually affects oxidative plant status and antioxidant action pathways (Silva et al. 2019).

Nanoparticles interact with plants causing many morphological and physiological changes, depending on the type of nanoparticles and their properties, but also plant species and their stage of development, time, doses and exposure methods. Research has been conducted to highlight the importance of considering the methods of preparing exposure solutions. In fact, the latter gives rise to size distributions and the different toxicological properties of nanoparticles (Tripathi et al. 2017; Jahan et al. 2018; Ogunkunle et al. 2020).

Disruption of photosynthetic activity leads to oxidative stress in plants, as photosynthetic efficiency is a functional factor for identifying biotic and abiotic stresses. NPs interfere and alter plant photosynthesis efficiency, photochemical fluorescence and quantum yield (Khatri and Rathore 2018); thus, the understanding of NPs-induced oxidative stress and plant antioxidant defense requires knowledge of NPs interactions with photosynthetic mechanism (Wu et al. 2017).

A related study showed that TiO_2 NPs (23 ± 1.6 nm) triggered modifications in metabolism, antioxidant enzyme activities and the generation of oxidative stress. The degree of alterations induced by NPs exposure is dependent on plant materials, plant compartments, exposure time and NPs doses (Missaoui et al. 2018). Castiglione et al. (2016) suggested that the antioxidant response in *faba bean* leaves increased after exposure to NPs, which depends largely on particle diameter. The effects of NPs in wheat plants depended on the plant organ, improving total antioxidant activity (TAA) in leaves but with malondialdehyde (MDA) increase, whereas in roots both MDA and TAA levels decreased (Silva et al. 2017).

In this context, this paper analyses TiO_2 nanoparticle risk on fenugreek (*Trigonella foenum graecum* L) growth for a period of 16 days. Also, the paper aims to give a comprehensive account of the mechanism of action of TiO_2 NPs (at size 83 ± 15 nm) in relation to chloroplast, mitochondria and cytosolic redox changes in fenugreek plants. The present study showed that the TiO_2 NPs, characterized by a spheric form, do not affect seedling growth and pigment. We have also showed the significant effect of TiO_2 on the oxidation of plant membranes and disorder in levels of organic compounds.

2 Materials and Methods

2.1 TiO_2 Nanoparticles Dispersion and Characterization

TiO_2 NPs suspensions (50 or 100 mg L^{-1}) were obtained from commercial nanopowder (Reagents Chemicals and Metals, Korea) by dispersing nanoparticles by agitation in Milli-Q water. The morphology was determined by drying 6 μL of the TiO_2 stock suspension on a glass slide and viewing the suspension using a scanning electron microscope (SEM) (Philips XL30SFEG). The X-ray diffraction (XRD) approach describes the nanoparticle's crystalline properties (X'Pert Pro Panalytical diffractometer). A Perkin-Elmer (FTIR 2000) spectrometer measured infrared spectrum using KBr pellets in the 4000–400 cm^{-1} region. Dynamic Light Scattering (DLS) measurements are sensitive to the concentration of NPs in suspensions, so a too low concentration of NPs generates fluctuations in intensity due to the diffusion of the particles in the suspension. These fluctuations are not taken into account in the model and are interpreted by the measuring device as large particles. Conversely, a too high concentration gives rise to multiple diffusion phenomena, also not taken into account in the model. These multiple diffusions lead to a decrease in the apparent diameter of the particles and to a higher polydispersity of the suspension (www.malven.com) in a first step. We therefore determined the optimal concentration of the suspension of NPs that allowed us to obtain precise hydrodynamic diameter measurements. These tests were performed with NPs suspended at different concentrations (Table 1). All analyses were made at room temperature.

2.2 Plant Material, Growth, and Treatment Conditions

Seeds were obtained from the Green Company -Tunis. The seeds were first disinfected for 10 min with sodium hypochlorite (2%), were washed thoroughly to eliminate the disinfectant's traces and soaked thoroughly for 24 h in distilled water at 4 °C to get an initial level. Twenty seeds were germinated on 9-cm diameter Petri dishes containing two sheets of filter paper moistened with 10 mL distilled water for 3 days in the dark at 24–26 °C. After germination, the seedlings used had similar length. These fenugreek plants were transferred to pots containing Hoagland's nutrient solution (1 L) with 50 or 100 mg L^{-1} of TiO_2 NPs treatments. Concentrations of TiO_2 NPs in solutions were dissolved for 60 min by the ultrasonic method and deposited in the dark (see Table 2). Seedling conditions were set to 25 °C, 70% relative humidity and light-dark 16:8 h. Continuous aeration for the plants is provided by modular aerators. After that, every 4 days up to 16 days, together with the control, the exposed seedlings were properly rinsed with distilled water to eliminate residues of nanoparticles and nutrients in the region. During experience, nutrient solutions were changed every 4 days. At the greenhouse stage, a research was carried out with five replications, and each pot contained 40 seeds (Missaoui et al. 2017).

Table 1 Particle size quantification of TiO_2 NPs Stock suspension determined by dynamic light scattering (DLS) using a Malvern (zetasizer nano-ZS) particle analyzer

Concentration of TiO_2 (mg/L)	**50**	**100**	**500**	**1000**
Hydrodynamic size (nm)	**96.4**	**154.8**	**172.4**	**266.4**

Table 2 Protocol of Hoagland nutrient solution preparation

Solution A: microelements solution
2.8 g H_2BO_2
3.4 g $MnSO_4$, H2O
100 mg $CuSO_4,5H_2O$
220 mg $ZnSO_4,7H_2O$
100 mg $(NH_4)_6MO_7O_{24},4H_2O$
Adjust the volume to 1 L with distilled water.
Store at 4 °C
Solution B
1 mL of concentrated H_2SO_4
Adjust the volume to 200 mL with distilled water.
Store at 4 °C
Solution C
7.44 g $Na_2EDTA,2H_2O$
10.2 g $FeSO_4,7H_2O$
Make up the volume to about 800 ml
Heat the solution to 70 °C in the dark, until a yellow-brown color is obtained.
Allow to cool, and adjust the volume to 1 L with distilled water.
Store at 4 °C
Hoagland stock solution (10x)
9.4 g Ca $(NO_3)_2,4H_2O$
5.2 g $MgSO_4,7H_2O$
6.6 g $KNO_2,7H_2O$
1.2 g KH_2PO_4
10 mL of solution A
1 mL of solution B
Adjust the volume to 1 L with distilled water.
Store at 4 °C.
Diluted Hoagland solution (1x)
100 mL stock solution (10x)
5 mL of solution C
Adjust the volume to 1 L with distilled water.
Prepare this solution extemporaneously.

2.3 Measurement of Seedling Growth and Biomass

Every 4 days, the seedlings are peeled, then separated into stems, leaves and roots. They were then quickly rinsed in three successive baths of distilled water and dried between two sheets of filter paper, then weighed to measure their fresh weight. The length of the stems, roots and internodes were determined by a 0.5 mm ruler. All weights were performed using a Sartorius precision balance with a precision of 0.1 mg. Seedlings were also used for specific physiological and biochemical studies, such as growth of seedlings, pigment levels and antioxidant enzyme activities, MDA content and nicotinamide adenine dinucleotide oxidase (NADH) activity. At harvest, seedlings were divided into leaves, stems and roots, and kept for biochemical studies in ultra-deep freezer at −80 °C. Samples for mineral analysis were dried.

2.4 Analysis of Metabolites

2.4.1 FTIR Analysis

Preparation of samples was defined by Naumann et al. (1991). The samples (leaves, stem and roots of *Trigonella foenum-graecum* L.) were dried in an oven at 70 °C for at least 8 days and

then mixed with 2.5 mg of dry potassium bromide (KBr) using a pestle. All FTIR spectra were obtained using Fourier Transform Infrared Spectrometer (Shimadzu) at room temperature (26 °C ± 1 °C) within the mid-infrared range (4000–500 cm^{-1}).

2.4.2 Quantification of Pigment Content

Using the method described by Arnon (1949), the photosynthetic pigments, namely chlorophyll-a (Chla) and -b (Chlb), and carotenoid content (Car) were estimated. Fresh leaves (100 mg) were ground using mortar with 5 mL of 80% (*v*/v) ice-cold acetone. The pigment extract was measured against an 80% (v/v) blank acetone at 647 and 663 nm wavelengths (A647-A663) for chlorophyll assays and 470 for carotene wavelengths (A470). Chlorophyll-a and -b, and carotenoid content were determined using the equations proposed by Lichtenthaler (Lichtenthaler and Wellburn 1983) and expressed as mg g^{-1} Fresh Weight.

$$\text{Chla}\ (\mu g/mL) = 12.21\ A663 - 2.81\ A646 \quad (1)$$

$$\text{Chlb}\ (\mu g/mL) = 20.13\ A646 - 5.03\ A663 \quad (2)$$

$$\text{Car}\ (\mu g/mL) = (1000\ A470 - 3.27\ \text{Chla} - 104\ \text{Chl b})/229 \quad (3)$$

2.4.3 Measurement of Anthocyanin Levels

Anthocyanin levels were measured according to Gould et al. (2000). To determine the anthocyanin content, fresh leaves were immediately soaked in acidified methanol (methanol: water:HCl = 16:3:1). Tissues were mixed using glass pestle and kept in the dark at 25 °C for 72 h. Spectrophotometrically, relative amount of anthocyanin was estimated at 530 and 653 nm wavelengths (A530-A653). Measurement of contents of anthocyanins was expressed as μg g^{-1} Fresh Weight. Finally, the following formula was used to calculate the quantities of the anthocyanin:

$$\text{Anthocyanin}\ (\mu g/mL) = A530 - 0.24A653 \quad (4)$$

2.4.4 Determination of Total Flavonoid and Phenolic

5 g of powder was added into 100 mL of boiling water after drying at 60 °C in an oven for 72 h. Sample was filtered after 15 min, and the filtrate was set to 100 mL with distilled water (Zayneb et al. 2015). Total flavonoids were calculated using the recorded aluminum chloride method (Zhishen et al. 1999). 4 mL of H_2O and 0.3 mL of $NaNO_2$ (5%) were added to 1 mL of the extract. 0.3 mL of $AlCl_3$ (10%) was added after 5 min, followed by 2 mL of NaOH (1 M). Final volume was made with H_2O up to 10 mL, and the solution was mixed. We read absorbance at 510 nm. Quercetin was used as the standard.

Total phenols were determined using the Folin Ciocalteu method reported by Singleton and Ross (Singleton and Rossi 1965). Briefly, 1 mL of Folin Ciocalteu reagent diluted 10 times and 0.8 mL of sodium carbonate 7.5% were added to 200 μL of the extract. Reaction mixture was left for 30 min, and the absorbance was measured at 765 nm. Gallic acid was used as the standard.

2.5 Estimation of Lipid Peroxidation

Malondialdehyde was calculated to assess lipid peroxidation (Hernández and Almansa 2002). Fresh tissues (250 mg) were ground with a mortar and pestle in a 2.5 mL of trichloroacetic acid (TCA) (0.1%). The homogenate was centrifuged at 800×g for 5 min. The resulting supernatant was centrifuged again at 1500×g for 10 min. The pellet was washed with the TCA (0.1%) (*w*/*v* = 1/5) and referred to as "chloroplast portion". Mitochondria from supernatant were sedimented by centrifuging at 20,000×g for 30 min. The supernatant obtained was carefully decanted and designated as "cytosol fraction". The pellet was resuspended in the TCA (0.1%) (w/v = 1/5) and referred to as "mitochondrial fraction" (Smiri et al. 2009). All operations were performed at 4 °C. A 0.5 mL aliquot of the extract was mixed with 1.5 mL of 0.5% of thiobarbituric acid (TBA) prepared in TCA (20%), and incubated at 90 °C for 20 min. Samples were centrifuged at 10000×g for 5 min after stopping the reaction in an ice bath. Homogenate absorbance was measured then at 532 nm. After the non-specific absorbance was subtracted at 600 nm, the MDA concentration was estimated using the extinction coefficient (155 mM^{-1} cm^{-1}).

2.6 Isolation of Cell Organelles from Fenugreek Seedlings

Fresh tissues were ground with a mortar and pestle in a homogenization medium (pH 8.0) consisting of 50 mmol L^{-1} Tris-HCl, 0.4 mol L^{-1} saccharose, 5 mmol L^{-1} EDTA-Na_2. (*w*/*v* = 1/3). The homogenate centrifuged at 800×g for 5 min. The resulting supernatant was centrifuged again at 1500 g for 20 min. Pellet was washed with the homogenization medium (*w*/*v* = 1/2) and referred to as "chloroplast portion". Mitochondria from supernatant were sedimented by centrifuging it at 20,000×g for 30 min. The supernatant obtained was carefully decanted and designated as "cytosol fraction". The pellet was washed with the homogenization medium (pH 8.0) consisting of 50 mmol L-1 Tris-HCl, 0.4 mol L-1 saccharose (w/v = 1/2) and referred to as "mitochondrial fraction". All operations were performed at 4 °C. The enzyme activities were (U /g Fresh Weight) calculated according to the following equation:

$$\text{Enzymes activities} = (\Delta A/\text{min})/\zeta \times (\text{Vt}/\text{Vext}) \times \text{R} \quad (5)$$

where ΔA: Absorbance of reaction mixture; ζ: Molar extinction coefficient; Vext: Enzyme extract; Vt: Total reaction volume in assay; R: ratio of fresh material to buffer volume.

2.6.1 Estimation of NADH Oxidase Activity (EC 1.6.99.3)

NADH oxidase activity was measured from the reduction in absorbance at 340 nm, with an extinction coefficient of 6.22 mM^{-1} cm^{-1} by the method of Ishida et al. (1987). NADH oxidase activity was measured in test sample mixture containing 100 mM sodium acetate (pH 6.5), 1 mM $MnCl_2$, 0.5 mM p-coumaric acid, 0.2 mM NADH and enzyme extract. The NADH oxidase activity was determined using a UV-Visible spectrophotometer (Lamba 2, PerkinElmer).

2.6.2 Estimation of Guaiacol Peroxidase Activity (EC 1.11.1.7)

According to the Fielding and Hall Protocol (Fielding and Hall 1978), guaiacol peroxidase activity was measured by following the H_2O_2 based oxidation of guaiacol. Enzyme extract was applied to 50 mm potassium phosphate (pH 7.0), 10 mM H_2O_2, 9 mM guaiacol reaction

mixture. The GPOX activity was computed using the extinction coefficient of 26.6 mM^{-1} cm^{-1}.

2.6.3 Estimation of Catalase Activity (CAT, EC 1.11.1.6)

Catalase enzyme activity was calculated by recording hydrogen peroxide decomposition according to Aebi protocol (Aebi 1984). Enzyme extract containing 50 mM potassium phosphate buffer (pH 7.0), 10 mM H_2O_2, 1 mM dithiothreitol (DTT) was applied to the reaction mixture. Enzyme activity was quantified by taking a UV-Visible spectrophotometer to measure diminished absorbance at 240 nm. CAT activity was computed using the extinction coefficient of 39.4 Mm^{-1} cm^{-1}.

2.6.4 Estimation of Ascorbate Peroxidase (EC 1.11.1.11)

Ascorbate peroxidase activity was calculated by the Nakano and Asada (1981) method from a reduction in absorbance at 290 nm (extinction coefficient of 2.8 mM^{-1} cm^{-1}). Reaction mixture contained 50 mM potassium phosphate (pH 7.0), 0.5 mM ascorbate, 2 mM H_2O_2, 1 mM EDTA, and extract of the enzymes.

2.7 Statistical Analysis

All data were statistically analyzed using two-way Analysis of variance (ANOVA), and the means were separate using Newman–Keuls multiple-range test (Statistica 8, StatSoft Co., USA). Differences were considered significant at $p < 0.05$.

3 Results and Discussion

3.1 Structural and Morphology Study

X-ray diffraction (XRD) technique was used to identify the structure phase and the crystal size of titanium dioxide nanoparticle. The XRD spectrum of TiO_2 is shown in Fig. 1a. XRD results comported dominant peaks of TiO_2 nanoparticles corresponded to rutile (R) phase. The results were analyzed using Joint Committee on Powder Diffraction Standards (JCPDS) data (Niltharach et al. 2012). The findings suggest that the powder is pure, without any phase uncleanness. Additionally, the Debye-Scherer equation (Eq. 6) was used to calculate the average crystallite size D of the titanium dioxide nanoparticle (Klug and Alexande 1974):

$$D = \frac{k\,\lambda}{\beta\,cos\theta} \tag{6}$$

where k is the Scherer constant ($k = 0.89$), λ is the incident X-ray wavelength ($\lambda =$ 0.154056 nm), β is the peak with at half maximum, and θ is the Bragg diffraction angle.

The average particle size of the crystallite was estimated to be around 83 ± 15 nm. Figure 1b showed the FTIR spectra of TiO_2 NPs, which showed a broad absorption band persisting due to the Ti-O vibration between 800 and 450 cm^{-1}. TiO_2 NPs morphology was analyzed using the electron microscopy (SEM) scanning method. Figure 1c indicated that the nanoparticles were agglomerated. The anatomy was made of spheres. Particle size quantification of TiO_2

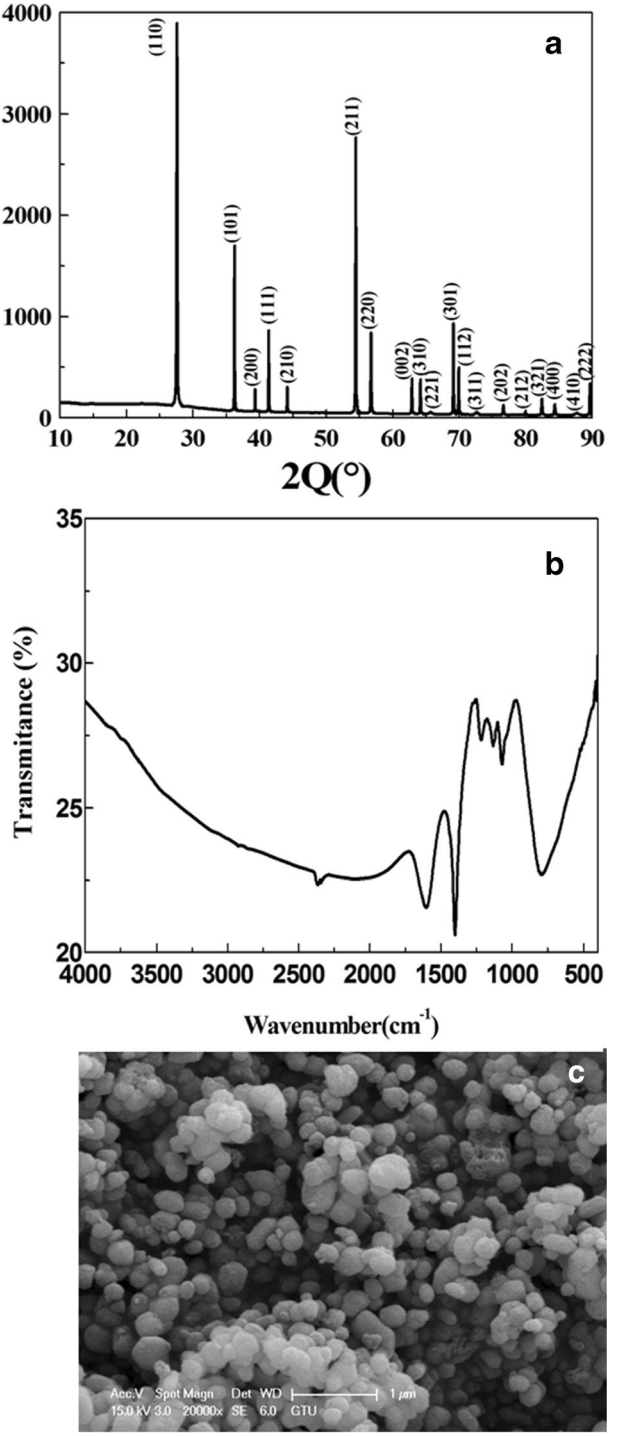

Fig. 1 **a** DRX, **b** FTIR and **c** SEM Analysis

NPs Stock suspension was determined by dynamic light scattering (DLS) using a Malvern (zetasizer nano-ZS) particle analyzer, and this analysis demonstrated an average particle size of 96.4 in the 50 mg L^{-1} stock TiO_2 NPs suspension (Table 1).

3.2 Development of Fenugreek

TiO_2 NPs had a major influence on stem growth (Table 4). TiO_2 NPs (100 mg L^{-1}) treatments had the longest stems, which reached 12 cm after 16 days of treatment. The 100 mg L^{-1} treatment showed an improvement of around 72% in the length of the stems relative to the control (Fig. 2a). Figure 2b showed that root lengths increased (by about 23%) after H_2O imbibition and TiO_2 NPs treatment. From Fig. 2c, d, it was evident that the internodes and the leaf area were enhanced after application of 100 mg L^{-1} TiO_2 NPs relative to the control (23% and 86%, respectively). From Fig. 2 it can be seen that TiO_2 NPs had a positive impact on plant morphology indicators. We can assume that interactive nanomaterials cause many morphological and anatomical variations depending on the nanoparticles' behavior and concentration (Siddiqui et al. 2015). The obtained results were in agreement with those from Jaberzadeh et al. (2013), who observed that TiO_2 NPs improve the growth and yield of wheat. Similar results were reported by Hussain et al. (2019), who affirmed that the biomass, leaf area, leaf thickness, Chla, Chlb, carotenoid, Ribulose-1,5—bisphosphate carboxylase/oxygenase (rubisco) activity, photochemical efficiency of photosystem II, and electron transport rate (ETR) of soybean increased at 2.5 mg Ti per plant. Also, Chemingui et al. (2019) reported that fenugreek treated with 5 and 50 mg L^{-1} of Zinc oxide nanoparticle showed an increase in the length of the stems by about 40% compared with control. However, Missaoui et al. (2017) showed that TiO_2 at size less than 20 nm caused disturbance of fenugreek growth and development, which was manifested by signs of toxicity (chloroses). In contrast to some reports in the literature, TiO_2 NPs (20 nm) at concentrations of 10 and 100 ppm increased the fresh weight of shoots and roots from wheat, while concentrations of less than 100 ppm of TiO_2 NPs decreased the fresh weight of manna (Vittori Antisari et al. 2014). Wu et al. (2017) showed that the biomass of rice was significantly decreased after exposure to nano-TiO_2. Also, Atha et al. (2012) have shown that copper oxide nanoparticles (CuO NPs) at size <100 nm decreased root growth of *Raphanus sativus*.

3.3 Metabolism of Polysaccharides, Lipids, Proteins, Pectin, Suberin and Lignin Molecules

The FTIR spectra of leaves treated with TiO_2 NPs did not show any apparent new peaks compared to controls (Fig. 3a; Table 3). Nevertheless, the peaks in 1300 to 1480 cm^{-1} range are typical of CH deformation and C — O stretching in the suberin and cutin outer surface. These peaks occurred in leaves exposed to 50 and 100 mg L^{-1} at a higher intensity than controls. In the region of 1630 and 1605 cm^{-1}, bands were characterized by carboxylate COOH and pectin. Band spectra from this area are not present in treated stems. Nonetheless, higher intensities were observed in the stress exposed to 50 and 100 mL^{-1} compared with controls (Fig. 3b; Table 3). In the region of peaks between 3350 and 3450 cm^{-1}, bands corresponded to O—H stretching in various polysaccharides and alcohols, peaks between 2930 and 2910 cm^{-1} correlated to asymmetric CH_2 molecules in lipids, lignin was traced in peaks between 1150 and 1060 cm^{-1}, the protein was assigned to bands between 1664 and 1648 cm^{-1}. Band spectra from these regions appeared in roots treated with TiO_2 NPs, but not present in root controls. Peaks between 1630 and 1605 cm^{-1} corresponded to carboxylate COOH and pectin. Peaks spectra were not found in roots exposed to 50 and 100 mg L^{-1} of TiO_2 NPs (Fig. 3c;

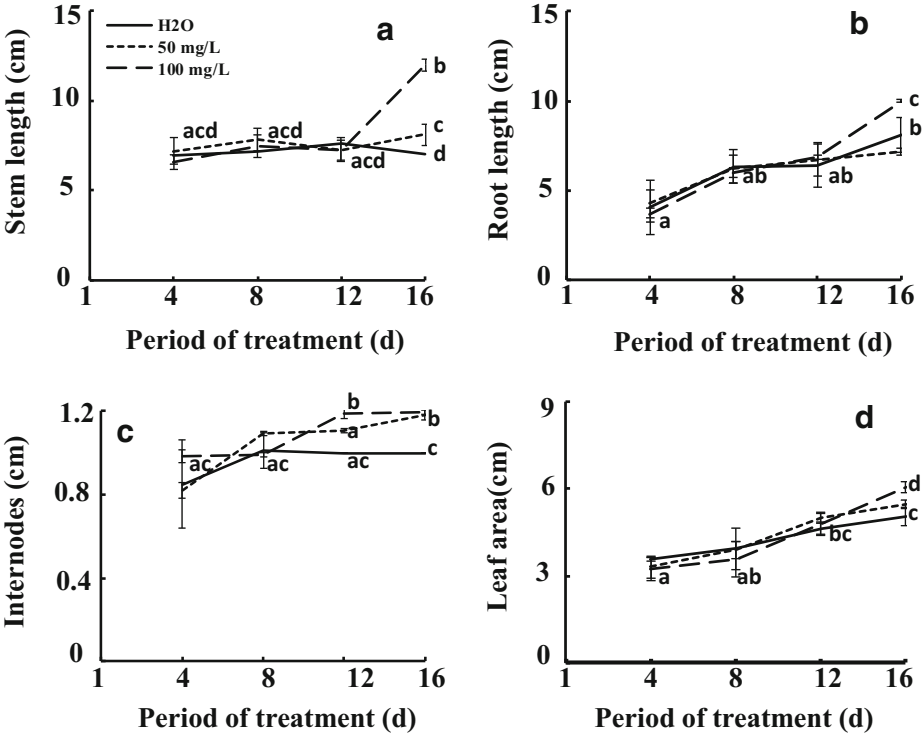

Fig. 2 Stem length (**a**), root length (**b**), internodes (**c**) and leaf area (**d**) of fenugreek in hydroponic media from control, 50 and 100 mg L^{-1} of TiO_2 NPs treatment. The values are the averages of 6 repetitions (±SE). Different letters represent significant differences between the treatment means. Differences were considered significant at $p < 0.05$ level

Table 3 and 4). This work gives insights into the biosynthesis mechanisms and the deposition of cell-wall-based plant structures in various plant organs after TiO_2 NPs exposure (Missaoui et al. 2018). The results offered by Piro et al. (2003) suggest that altered stress may lead to changes in the biosynthesis of cell wall polysaccharides in roots isolated from treated and untreated wheat seedlings (*Triticum durum Desf.*). TiO_2 NPs were observed to adsorb on the root cell membrane, where they would then infiltrate cells and interact with biomolecules, including proteins, lipids and other cellular biomolecules. Data revealed chemical modifications in fenugreek's leaves, stems and roots. Such findings are in agreement with other studies that showed that cerium dioxide (CeO_2) nanoparticles had modified the nutritional qualities of *Coriandrum sativum* L. (cilantro) (Morales et al. 2013). Similarly, Zuverza-mena et al. (2016) also found variations in the bands that refer to plant cell lipids, proteins, and structural components, such as lignin, pectin, and cellulose. In addition, development, nutritional value, and macromolecule conformation have been impacted after application of silver nanoparticles (Ag NPs) on radish sprouts (Zuverza-mena et al. 2016).

3.4 Metabolism of Pigments

Figure 4a, b shows a significant enhancement in Chla (59%) and Chlb (87%) in fenugreek leaves after treatment with 100 mg L^{-1} TiO_2 NPs relative to the control. No further significant changes in carotenoids and anthocyanins were observed at the later stage (16 days) of nano-

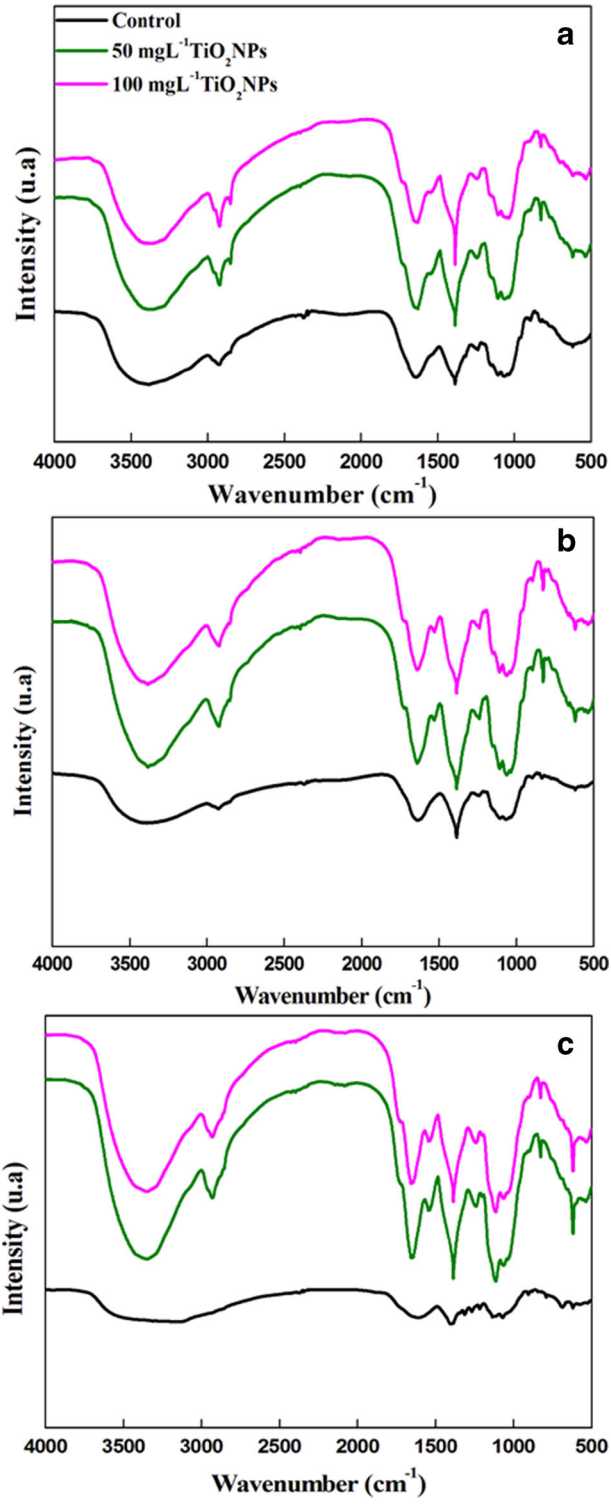

Fig. 3 FTIR bands spectra of leaves (**a**), stem (**b**) and root (**c**) of fenugreek (*Trigonella foenum-graecum* L.) treated with TiO_2 NPs [0, control; 50 and 100 mg L^{-1}]

Table 3 FTIR Vibrational Shifts on bands of leaves, stem and root of *Trigonella foenum-graecum* L. treated with TiO_2 NPs [0, control; 50 and 100 mg L^{-1}]

Reference	Literature frequency (cm^{-1})	Functional group	Assignment	Frequency (cm^{-1})								
				Leaves			Stems			Roots		
TiO_2 NPs treatments mg L^{-1}				Control	50	100	Control	50	100	Control	50	100
[1]	3300–3400	OH stretch	Various polysaccharides, alcohols	3398	3379	3391	3400	3383	3391	–	3366	3385
[2]	2930–2910	CH_2 asymmetric	Lipids	2916	2930	2918	2918	2918	2920	–	2922	2922
[2]	1630–1605	COOH	Carboxylate COOH, pectin	1630	1630	1630	1630	–	–	1611	–	–
[2]	1664–1648	C=O, C-N	Protein	1648	1648	1648	1648	1648	1648	–	1648	1648
[2]	1300–1480	CH deformation and C–O stretch	Outer surface suberin/cutin	1390	1381	1382	1386	1374	1381	1395	1383	1376
[2]	1150–1060	C-O-C (ether)	Lignin	1070	1074	1068	1088	1074	1082	–	1110	1110

[1] Lammers et al. (2009); [2] Zuverza-mena et al. (2016)

Table 4 Effects of 50 and 100 mg L^{-1} of TiO_2 NPs on GPOX, CAT and APX activities in chloroplast (CH), mitochondria (M) and cytosol (C) of leaves, stems and roots of *Trigonella foenum-graecum* L. Data are means (± SE) of three replicates. Values with asterisks are significantly different at $p < 0.05$

Days (d)			4	8	12	16
Plant part	**Fractions**	**Treatments mg L^{-1}**				
GPOX						
Leaves	**CH**	**0**	**0.33±0.05***	**0.94±0.24**	**1.02±0.24**	**1.03±0.05***
		50	**1.2±0.07***	**0.8±0.06**	**0.6± 0,07**	**0.75±0.07***
		100	**0.9±0.09***	**0.4±0.01**	**0.8±0.08**	**0.7±0.02***
Stem		**0**	**0.96±0.12***	**1.45±0.1***	**1.3±0.15***	**1.2±0.13***
		50	**0.27±0.06***	**0.27±0.09***	**0.4±0.04***	**0.6±0.12***
		100	**0.12±0.03***	**0.22±0.03***	**0.22±0.07***	**0.2±0.08***
Leaves	**M**	**0**	**0.96±0.08**	**0.7±0.05**	**0.9±0.07**	**1.3±0.2***
		50	**0. 5±0.05**	**0.2±0.05**	**0.44±0.07**	**0.6±0.08***
		100	**0.35±0.01**	**0.34±0.02**	**0.16±0.09**	**0.14±0.07***
Stem		**0**	**0.3±0.08**	**0.3±0.08**	**0.33±0.06**	**0.32±0.07**
		50	**0.14±0.25**	**0.31±0.02**	**0.3±0.06**	**0.4±6.10–3**
		100	**0.14±0.05**	**0.13±0.01**	**0.23±0.06**	**0.26±0.025**
Root		**0**	**1.3±0.14***	**1.1±0.17**	**1.1±0.18**	**1.2±0.14***
		50	**0.4±0.06***	**0.42±0.03**	**1.3±0.07**	**0.7±0.08***
		100	**0.3±0.11***	**0.4±0.11**	**0.3±0.06**	**0.8±0.08***
Leaves	**C**	**0**	**0.34±0.06***	**0. 5±0.08***	**0. 5±0.1***	**0.64±0.08***
		50	**1.7±0.21***	**2.3±0.1***	**2.1±0.07***	**3.9±0.26***
		100	**1.7±0.3***	**1.6±0.2***	**2.7±0.08***	**2.1±0.08***
Stem		**0**	**0.8±0.13**	**0.92±0.2**	**0.7±0.12**	**0.8±0.05***
		50	**1±0.09**	**0.8±0.11**	**0.8±0.14**	**0.9±0.08***
		100	**0.3±0.06**	**1.2±0.03**	**1.6±0.09**	**1.8±0.1***
Root		**0**	**0.43±0.08***	**0.43±0.06***	**0.41±0.04 ***	**0.42±0.07***
		50	**2.82±0.08***	**0.3±0.5***	**4±0.5***	**4.7±0.6***
		100	**3.3±0.15***	**4.6±0.6***	**5.3±0.5***	**4. 9±0.8***
CAT						
Leaves	**CH**	**0**	**0.09 ± 7.10^{-4}**	**0.02 ± 7.10^{-4}**	**0.01 ± 3.10^{-3}**	**0.02 ± 5.10^{-3} ***
		50	**0.04±0.02**	**0.3±0.1**	**0.21 ± 9.10^{-3}**	**0.16±0.02***
		100	**0.1 ± 5.10^{-3}**	**0.1±0.05**	**0.3±0.07**	**0.2±0.06***
Stem		**0**	**0.03 ± 4.10^{-4}**	**0.04 ± 6.10^{-3}**	**0.05 ± 6.10^{-3}**	**0.05 ± 7.10^{-3} ***
		50	**0.6±0.03***	**0.8±0.09**	**1.22±0.3**	**3.2±0.2***
		100	**0.04±10–3 ***	**0.23±0.08**	**0.68±0.2**	**1.2±0.06***
Leaves	**M**	**0**	**0.014 ± 5.10^{-3}**	**0.04 ± 10^{-3}**	**0.03 ± 2.10^{-4}**	**0.03 ± 6.10^{-4}**
		50	**0.33 ± 7.10^{-3}**	**0.4±0.08**	**0.42±0.1**	**0.4±0.1**
		100	**0.25±0.06**	**0.2±0.06**	**0.2±0.01**	**0.24±0.05**
Stem		**0**	**0.12±0.02**	**0.12 ± 4.10^{-3}**	**0.18 ± 2.10^{-3}**	**86.9 ± 2.10^{-3} ***
		50	**0.2±0.02**	**0.25±0.04**	**0.33±0.05**	**88.5±0.13***
		100	**0.34±0.1**	**0.2±0.1**	**0.3±0.03**	**83.3±0.02***
Root		**0**	**0.3 ± 8.10^{-3} ***	**0.4±0.03**	**0.2±0.03**	**0.2±0.03***
		50	**1.6±0.07 ***	**1.7±0.1**	**1.4±0.04**	**1±0.05***
		100	**0.7±0.1***	**0.3±0.08**	**0.45±0.03**	**0.6±0.05***
Leaves	**C**	**0**	**0.9±0.05**	**1±0.032**	**1.04±0.05**	**1.1±0.03***
		50	**0.2±0.08**	**0.4±0.16**	**0.6±0.24**	**0.41±0.06***
		100	**0.32±0.04**	**0.9±0. 5**	**1.5±0.3**	**1.1±0.5***
Stem		**0**	**0.22±0.03**	**0.11 ± 10^{-5}**	**0.13±0.02**	**0.06 ± 3.10^{-3} ***
		50	**0.2±0.01**	**0.2±0.03**	**0.4±0.11**	**0.6±0.05***
		100	**0.4±0.2**	**0.62±0.04**	**0.26±0.03**	**0.6±0.12***
Root		**0**	**0.4±0.09**	**0.39±0.06**	**0.38±0.06**	**0.35±0.02***
		50	**0.8±0.2**	**0.51±0.3**	**0.8±0.3**	**1±0.08***
		100	**0.3±0.02**	**1.3±0.46**	**0.38±0.04**	**0.8±0.3***
APX						
Leaves	**CH**	**0**	**0.9±0.05**	**0.3 ± 3.10^{-3}**	**0.8±0.06**	**0.7±0.05**

Table 4 (continued)

Days (d)			4	8	12	16
Plant part	**Fractions**	**Treatments mg L^{-1}**				
		50	**0.5±0.1**	**0.7±0.2**	**0.8± 0,15**	**0.9±0.3**
		100	**1±0.12**	**1.4±0.19**	**1.5±0.34**	**1.44±0.3**
Stem		**0**	**1.5±0.01**	**0.7±0.21**	**0.8±0.03**	**0.42±5.10^{-7} ***
		50	**1.8±0.02**	**0.9±0.5**	**0.9±0.5**	**1.3±0.5***
		100	**1.5±0.3**	**0.8±0.4**	**0.8±0.2**	**1.5±0.2***
Leaves	**M**	**0**	**0.4±0.03***	**0.2±3.10^{-3}***	**0.35±0.14***	**0.11±0.04***
		50	**12.9±1***	**13.2±3.3***	**13.5±2.4***	**16.8±0.2***
		100	**12.9±1.6***	**17.1±0.033***	**17.7±0.85***	**14.7±2.5***
Stem		**0**	**1±0.05**	**1.7±0.13**	**1.2±0.14**	**1.9±0.24***
		50	**1.7±0.014**	**1±0.09**	**1.3±0.03**	**0.3±0.04***
		100	**2±0.07**	**0.42±0.13**	**0.6±0.25**	**1.7±0.5***
Root		**0**	**1.1±0.03***	**1.2±0.1***	**1.1±0.2***	**0.9±0.16***
		50	**14.2±2***	**14.8±1.15***	**18.15±1.9***	**14.53±1.75***
		100	**10±0.45***	**5.8±0.75***	**5.9±0.3***	**6.7±1.05***
Leaves	**C**	**0**	**0.8±0.04***	**0.3±0.02***	**0.25±4.10^{-3}***	**0.25±0.064***
		50	**12.75±2.5***	**11.3±3.4***	**24.9±5***	**22.8±0.5***
		100	**9.3±3.1***	**15.6±1.1***	**32.4±0.3***	**35.4±2***
Stem		**0**	**0.6±0.02**	**0.54±4.10–3 ***	**0.9±0.1***	**1±0.1***
		50	**9±0.4**	**9.3±0.2***	**20.7±0.3***	**28.2±7***
		100	**15.2±4.75**	**7.65±2.4***	**6.75±2.4***	**8.66±0.2***
Root		**0**	**9.7±4.7**	**13.3±1.99**	**6.3±1.6**	**5.3±0.25**
		50	**5.3±3.1**	**2.8±5.9**	**4.8±0.7**	**4.7±1.35**
		100	**6.15±3.4**	**8.9±2.86**	**6.6±1.3**	**9.22±3.8**

stress (Fig. 4c, d). At 16 days of stress, all nanostressed leaves exhibited significantly diminished flavanoids level (60%), but accumulated polyphenols (17–56%). The results show that flavonoids and polyphenols levels of stem were significantly declined (95%) compared with controls (Fig. 4e, f).

These results show that the addition of TiO_2 NPs at size 83 nm induced the photosynthetic parameters (accumulation of chlorophylls and enhancement of leaf area). These responses vary depending on the dose. We recorded the highest responses for the highest doses of TiO_2 NPs. Scott (2014) showed that, due to its high refractive index and ultraviolet radiation attenuation, the TiO_2 NPs protected the plant from drought, heat stress, and sunburn, resulting in less damage to the plant. TiO_2 has a high UV-absorbing capacity, which, combined with its high refractive index, provides very high UV protection. In the same way, TiO_2 is also stable and does not discolor under the effect of UV light. In addition, TiO_2 is a photocatalyst under UV light (Scott 2014). Yang et al. (2006) concluded that TiO_2 NPs could improve chlorophyll structure and sunlight capture, promote pigment manufacturing and light energy transformation to active electron and chemical operation, and increase photosynthetic efficiency and induce the rubisco, which improves photosynthesis.

Juárez-Maldonado et al. (2019) had also found nanoparticles as biostimulants. Recently, several authors (Hong et al. 2005b; Hong et al. 2005a; Ma et al. 2013) have indicated that TiO_2 NPs improved light absorption and transformation from light energy to electrical and chemical energy, and also stimulated the assimilation of carbon dioxide by enabling rubisco carboxylation, preventing aging of chloroplasts and inducing the activation of rubisco genes. The effect of various concentrations of titanium dioxide nanoparticles was evaluated by Tighe-Neira et al. (2020), Shabbir et al. (2019) and Juárez-Maldonado et al. (2019). Interestingly, they observed

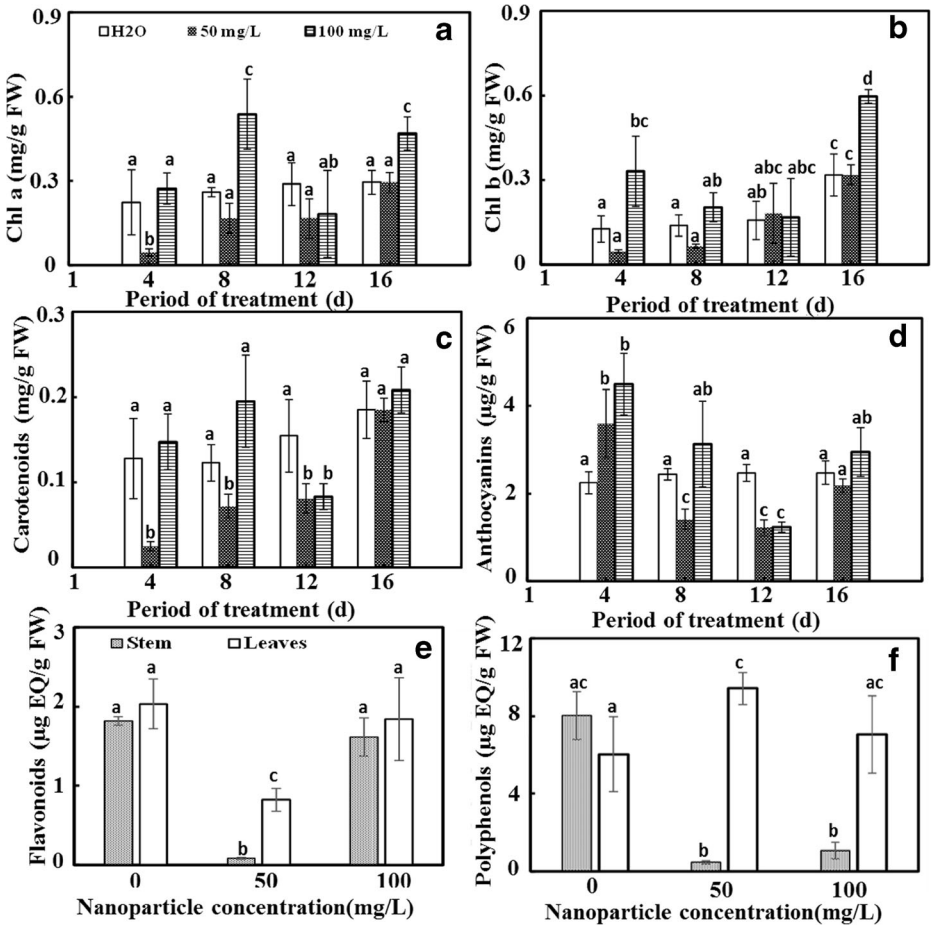

Fig. 4 Effects of 50 and 100 mg L^{-1} of TiO_2 NPs on the pigment (Chla (**a**), Chlb (**b**), carotenoids (**c**) and anthocyanins (**d**)) contents in leaves and on the flavonoid (**e**) and polyphenol (**f**) contents in leaves and stems of fenugreek (*Trigonella foenum-graecum* L.) over 16 days compared to control (H_2O). Data are means (± SE) of four replicates with one seedling each. Different letters represent significant differences between the treatment means. Differences were considered significant at $p < 0.05$ level

that the quantities of chlorophyll and the photosynthetic rate were substantially increased in treatments with TiO_2 NPs. The results offered by Morteza et al. (2013) noted that the impact of TiO_2 NPs was significant on chlorophyll content, total chlorophyll, chlorophyll a/b, carotenoids and anthocyanins.

Unlike some literature reports, it has been shown that in *Triticum aestivum* L., 5.0 g L^{-1} of TiO_2 NPs resulted in a significant decrease in chlorophyll contents and photosynthetic activity (Chen et al. 2019). Missaoui et al. (2017) observed that treatment with 100 mgL^{-1} of TiO_2 NPs at size less than 20 nm resulted in lower chlorophyll a, b, and carotenoids and chlorosis in the leaf area, and was concluded that the physiological effects are likely attributable to small particle size, which enables them to penetrate the plant during exposure. Size is a critical factor in assessing the effect of NPs on plants. We showed that TiO_2 NPs at size 83 ± 15 nm was

internalized to a smaller proportion than NPs with a diameter of 23 ± 1.6 nm (Missaoui et al. 2020, in press).

3.5 Chloroplast Redox Pathway

3.5.1 Installation of Oxidative Stress

Fig. 5a, b indicated that MDA activity from treated chloroplast of stems was substantially reduced compared to controls (70%), but no major effect was seen on chloroplast from leaves after TiO_2 NPs treatment. An important implication of these findings is that TiO_2 NPs treatment significantly decreased the accumulation of $O_2^{\bullet-}$ and H_2O_2, which resulted in marked decrease of lipid peroxidation. This was attributed to capacity of Ti^{4+}/Ti^{3+} to oxidize/reduce $O_2^{-}/O_2^{\bullet-}$ to O_2/H_2O_2 (Lei et al. 2008). However, the addition of TiO_2 NPs stimulated NADH oxidase activities from treated leaves chloroplast compared with controls (4-fold), but no further significant changes in NADH activities from stems were observed (Fig. 6a, b). The excessive NADH activity demonstrated the installation of the oxidative stress in TiO_2 NPs poisoned chloroplast of fenugreek leaves. Recently, Hong et al. (2017) identified the production of chloroplastic ROS in *S. polyrhiza* based on Ag NPs to inhibit rubisco activity and the photo-protective capacity of Photosystem II. Chloroplasts are the main sites of ROS production, and were especially vulnerable to excessive ROS generation (Silva et al. 2019).

3.5.2 The Antioxidant System

Table 3 shows that guaiacol peroxidase activity (GPOX) was significantly decreased in chloroplast from leaves and stems compared with controls (30% and 50–85%), but increased catalase (CAT) and ascorbate peroxidase (APX) activities in chloroplast from leaves and stems after TiO_2 NPs treatment. Enhancing CAT and APX activities may be due to TiO_2 NPs, which protects chloroplast from excessive light by induction of antioxidant enzyme activities (Hong et al. 2005b). This finding aligned with some earlier work proved that TiO_2 NPs acted as a photocatalyst and cause oxidation-reduction reaction (Crabtree 2000). Yang et al. (2006) published similar findings that TiO_2 NPs improved light absorbance, accelerated the transportation and transformation of light energy, protect chloroplasts from aging, and extended the chloroplasts photosynthetic period.

3.6 Mitochondrial Redox Pathway

3.6.1 Installation of Oxidative Stress

Even at 16 days of nano-stress, significantly enhance MDA activities from mitochondria stems (97%) and roots (141%) were recorded (Fig. 5d, e). Interestingly, long exposure of TiO_2 NPs stress had a significant effect in decline NADH oxidase activities from mitochondria of leaves (50%) and roots (55–76%) compared to controls (Fig. 6c, e). The results disagreed with our previous work (Missaoui et al. 2018), which reported that lipid peroxidation activities declined in mitochondria from leaves, stems and roots (30%, 92% and 73%, respectively). A decrease or increase in MDA levels can be attributed to two causes: (1) mitochondrial dysfunction caused by oxidative stress; and (2) protective effect of the antioxidant system. This contradiction can be due to the size of TiO_2 NPs. Faisal et al. (2016) demonstrated that, as a consequence of oxidative stress, Co_3O_4 caused DNA damage, mitochondrial dysfunction,

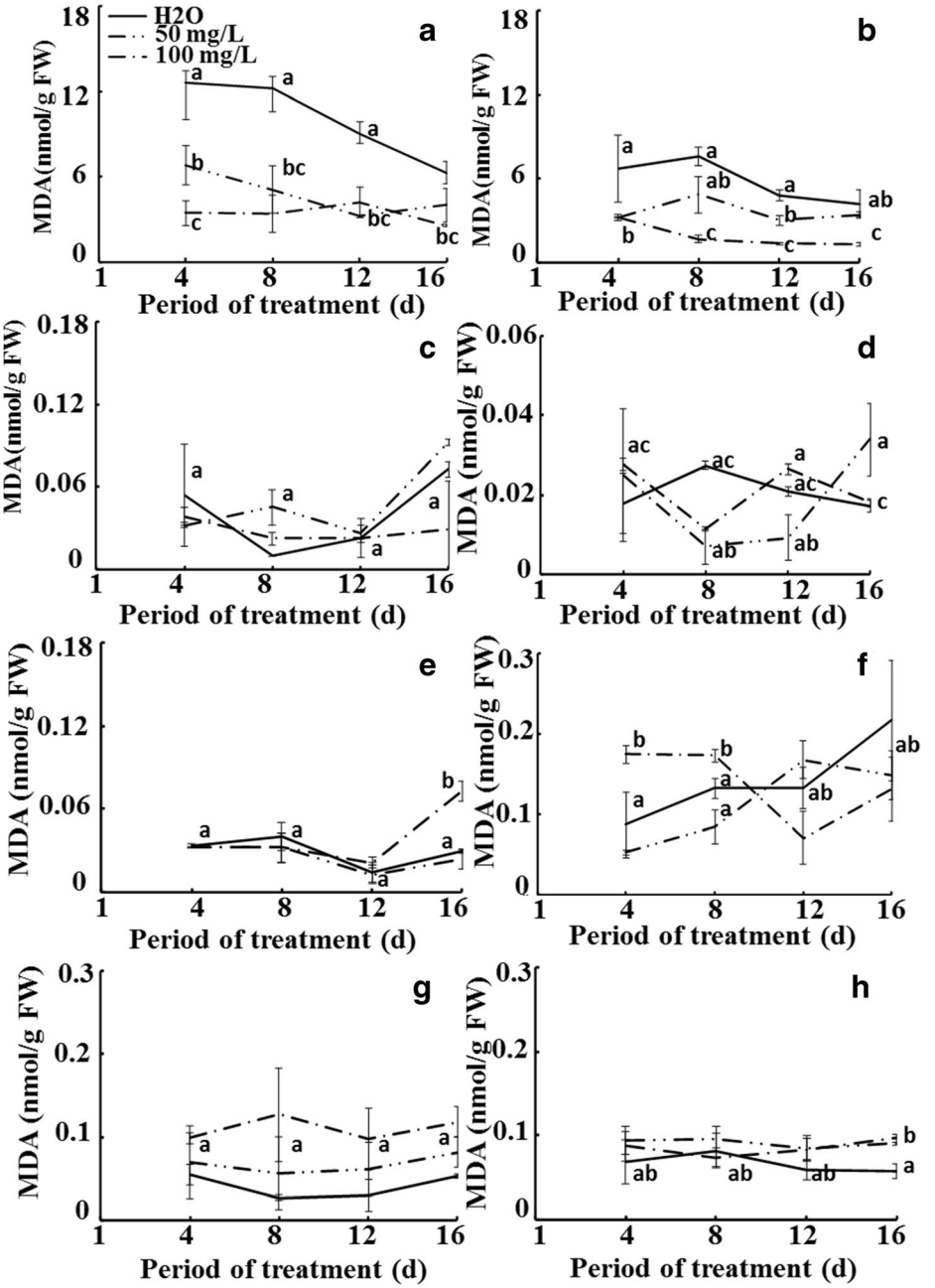

Fig. 5 Effects of 50 and 100 mg L^{-1} of TiO_2 NPs on MDA activity in chloroplast [Leaves (**a**) and Stem (**b**)], mitochondria [Leaves (**c**), Stem (**d**) and root (**e**)] and cytosol [Leaves (**f**), Stem (**g**) and root (**h**)] of fenugreek (*Trigonella foenum-graecum* L.) seedlings. Data are means (± SE) of three replicates. Different letters represent significant differences between the treatment means. Differences were considered significant at $p < 0.05$ level

and cell apoptosis in eggplants. Mitochondria play a significant function in the synthesis of adenosine triphosphate (ATP) and apoptosis.

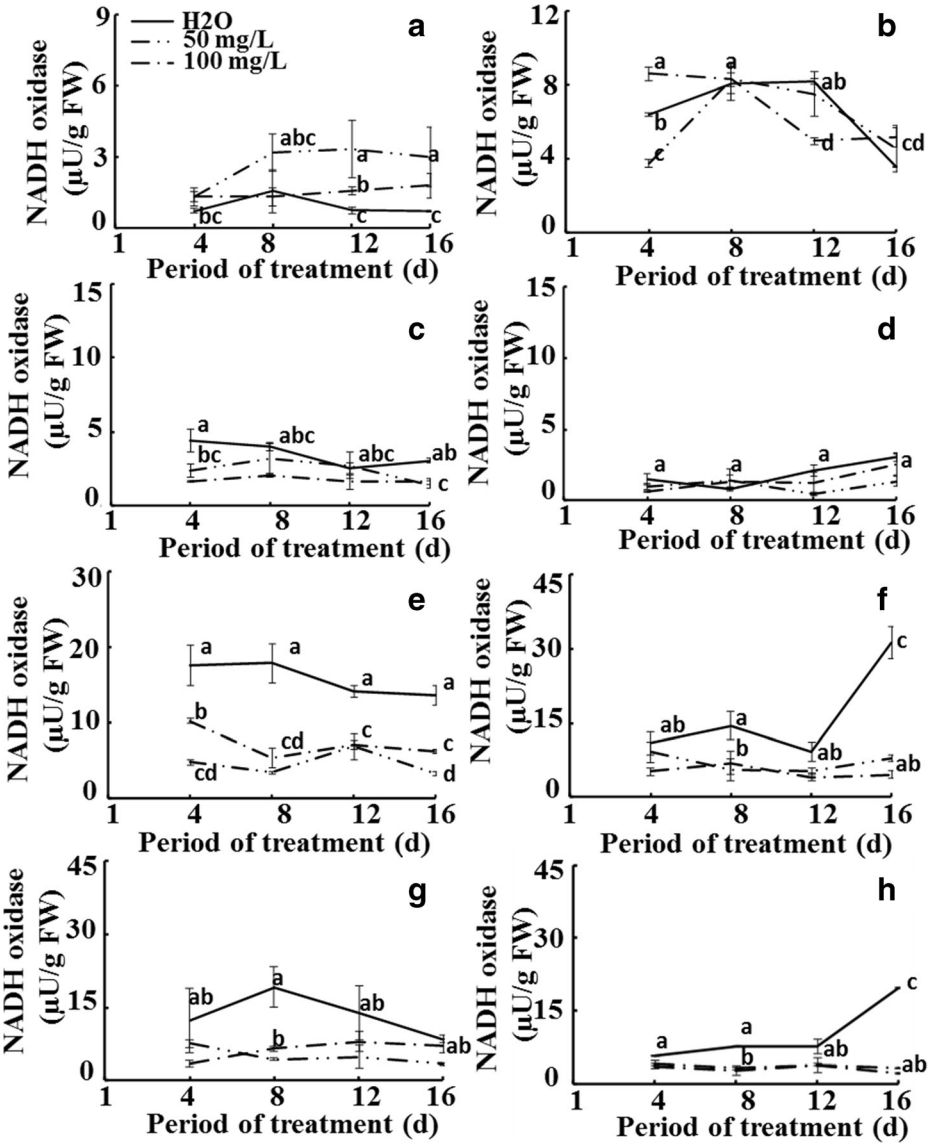

Fig. 6 Effects of 50 and 100 mg L^{-1} of TiO_2 NPs on NADH oxidase activity in chloroplast [Leaves (**a**) and Stem (**b**)], mitochondria [Leaves (**c**), Stem (**d**) and root (**e**)] and cytosol [Leaves (**f**), Stem (**g**) and root (**h**)] of fenugreek (*Trigonella foenum-graecum* L.) seedlings. Data are means (± SE) of three replicates. Different letters represent significant differences between the treatment means. Differences were considered significant at $p < 0.05$ level

Fröhlich et al. (Frohlich 2013) concluded that mitochondria are sensitive to nanomaterials exposure. Lesions were found when exposed cells to different particles. Lead et al. (2018) reassessed that nanomaterials do not tend to directly target mitochondria. Their susceptibility seems to be closely linked to their vulnerability to oxidative stress, which may be caused by interference of nanomaterials with the mitochondrial electron transport chain, or by their constituents. As Dai et al. (2018) reported, carbon nanotubes (CNTs) could be found in plant

cell mitochondria and reduced mitochondrial activity. Using direct interaction with mitochondria, CuO NPs may be internalized by plant cells and interrupt the mitochondrial electron transport chain, thereby induced over-generation of Reactive oxygen species (ROS) and oxidative stress (Dai et al. 2018).

3.6.2 The Antioxidant System

The addition of TiO_2 NPs inhibited GPOX activities from mitochondria of leaves and roots organs compared with controls (60–90% and 30–46%, respectively) but stimulated CAT and APX activities from mitochondria of leaves, stems and roots (Table 3). The obtained results were compatible with those of Dai et al. (2018), which reported that CAT activity was significantly decreased, which may be due to excessive generation of intracellular H_2O_2. The results were in agreement with those of Missaoui et al. (2018), which stated that antioxidant enzyme activity was altered significantly after treatment with NPs. From the data, it seems that variations in antioxidant responses depend on the size of NPs. This finding was in disagree with some earlier studies (Tripathi et al. 2017) reported that 50 mg L^{-1} TiO_2NPs did not affect antioxidant enzyme activity in *faba bean.*

3.7 Cytosolic Redox Pathway

3.7.1 Installation of Oxidative Stress

Notably, after 16 days of TiO_2 NP stress, no significant effect in MDA activities from cytosol of leaves and stems was observed, but MDA increased in cytosol of roots (62%) (Fig. 5f, g, h). Indirectly, nano-stress caused a gradual increase in H_2O_2 levels and MDA concentration due to oxidative stress (Missaoui et al. 2017). As compared to controls, NADH activities diminished in cytosol of leaves (85%) and root (89%) after TiO_2 NPs treatment (Fig. 6f, h). Hight NADH oxidase activities in tissues of fenugreek following exposure to TiO_2 NPs can be the source of oxidative stress. Wang et al. (2020) also reported that *Arabidopsis* exposed to 20 nm Ag NPs treatment at 50 mg L^{-1} caused oxidative stress. CeO_2 NPs did not change the accumulation of malondialdehyde (MDA) (Rico et al. 2013).

3.7.2 The Antioxidant System

100 mg L^{-1} TiO_2 NPs treatment stimulated GPOX activities from cytosol in leaves, stems and roots compared with controls (6, 2.3, 11-fold, respectively), and also stimulated APX activities from leaves and stems (141.28-fold) (Table 3). In leaves, CAT activity decreased significantly (62%) compared with controls, but increased in stems (11-fold) and roots (3-fold) after TiO_2 NPs treatment. Chahardoli et al. (2020) showed increase of some enzymes activities of antioxidant system (APX, CAT, superoxide dismutase (SOD) and peroxidase (POD)), mainly following exposure to 50–2500 mg L^{-1} of Al_2O_3 NPs and NiO NPs in roots and shoots of *Nigella arvensis* L. These findings are consistent with those of Hernandez-Viezcas et al. (2015), which showed that the production of cerium dioxide (CeO_2) nanoparticles at concentration of 2000 mg L^{-1} in mesquite roots generated a notable improvement in APX and CAT activities and hydrogen peroxide. In *Triticum aestivum* L. TiO_2 NPs at doses of 1.0 and 5.0 g L^{-1} increased antioxidant enzymes activities (Chen et al. 2019). Missaoui et al. (2018) found that the accumulation of Ti (TiO_2 NPs smaller than 20 nm) was detected in cytosol and

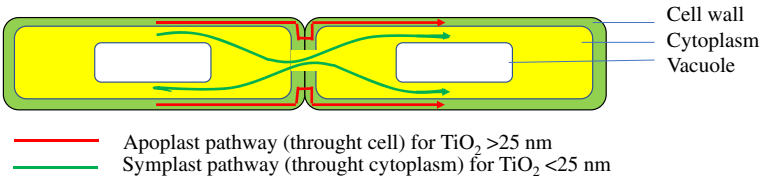

Fig. 7 Proposed mechanism for dysfunction of the transport canals for metabolites and nutrients during transport of TiO_2 NPs

mitochondria. So, TiO_2 at a size less than 20 nm has a direct effect on cytosol targets during the transport of NPs via symplast pathway. The effect of TiO_2 NPs at size 83 nm is indirect and could be due to the dysfunction of the transport canals for metabolites and nutrients during the transport of NPs via the apoplast pathway (Fig. 7).

4 Conclusions

TiO_2 nanoparticles have significant impact on plant metabolism. The TiO_2 NPs, characterized by the spheric form, at size of 83 nm did not affect seedling growth and photosynthesis. We have showed the significant effect of TiO_2 NPs on plant membranes by disorder in levels of organic compounds. Nanoparticles were accumulated and transported from roots to leaves in the most important plant cell parts. High lipid peroxidation and stimulation of oxidative stress due to NP treatment can be explained, in part, by accumulation of 83 nm nanoparticles within the plant cells. We observed that NPs induced MDA activities in mitochondria and cytosol, but not in chloroplast. Based on the correlations between mitochondria and cell apoptosis, accumulation of TiO_2 causes lipid peroxidation, redox changes, and finally, cell death. We proposed a model for TiO_2 NP transport in plant tissues and leaves of fenugreek seedlings. We suggested that TiO_2 NPs were accumulated in the cell wall, resulting in the closure of plant cell pores caused the suspension of functions of the most important organelle targets such as mitochondria.

Acknowledgments We thank Dr. Tawhida Akhter, Assistant Professor in the Department of English Language, Shaqra University Saudi Arabia, for check of language. We are thankful to the anonymous reviewers for helpful comments on the manuscript.

Authors' Contributions All authors contributed to the study conception and design. Material preparation, data collection and analysis were performed by [Takwa Missaoui], [Moez Smiri], [Hajer Chemingui] and [Amor Hafiane]. The first draft of the manuscript was written by [Takwa Missaoui] and all authors commented on previous versions of the manuscript. All authors read and approved the final manuscript.

Conceptualization: [Moez Smiri]; Methodology: [Takwa Missaoui], [Hajer Chemingui]; Formal analysis and investigation: [Takwa Missaoui], [Moez Smiri]; Writing - original draft preparation: [Takwa Missaoui], [Moez Smiri]; Writing - review and editing: [Amor Hafiane]; Funding acquisition: [Takwa Missaoui]; Resources: [Amor Hafiane]; Supervision: [Moez Smiri].

Funding No funding was received.

Data Availability All data generated or analyzed during this study are included in this published article.

Declarations

Disclosure of Interest The authors declare that they have no conflict of interest.

References

Aebi H (1984) Catalase in vitro. Methods Enzymol 105:121–126. https://doi.org/10.1016/S0076-6879(84)05016-3

Arnon D (1949) Copper enzymes in isolated chloroplasts, polyphenol oxidase in Beta vulgaris. Plant Physiol 2: 1–15. https://doi.org/10.1104/pp.24.1.1

Atha DH, Wang H, Petersen EJ, Cleveland D, Holbrook RD, Jaruga P, Dizdaroglu M, Xing B, Nelson BC (2012) Copper oxide nanoparticle mediated DNA damage in terrestrial plant models. Env Sci Technol 46: 1819–1827. https://doi.org/10.1021/es202660k7

Bundschuh M, Filser J, Lüderwald S, Mckee MS, Metreveli G, Schaumann GE, Schulz R, Wagner S (2018) Nanoparticles in the environment : where do we come from, where do we go to ? Environ Sci Eur 30:1–17. https://doi.org/10.1186/s12302-018-0132-6

Castiglione MR, Giorgetti L, Bellani L, Muccifora S, Bottega S, Spanò C (2016) Root responses to different types of TiO_2 nanoparticles and bulk counterpart in plant model system *Vicia faba* L. Env Exp Bot 130:11–21. https://doi.org/10.1016/j.envexpbot.2016.05.002

Chahardoli A, Naser K, Xingmao M, Farshad Q (2020) Effects of engineered aluminum and nickel oxide nanoparticles on the growth and antioxidant defense systems of *Nigella arvensis* L. Sci Rep 10:1–11. https://doi.org/10.1038/s41598-020-60841-6

Chemingui H, Smiri M, Missaoui T, Hafiane A (2019) Zinc oxide nanoparticles induced oxidative stress and changes in the photosynthetic apparatus in fenugreek (*Trigonella foenum graecum L.*). Bull Environ Contam Toxicol 102:477–485. https://doi.org/10.1007/s00128-019-02590-5

Chen Y, Wu N, Mao H, Zhou J, Su Y, Zhang Z, Zhang H, Yuan S (2019) Different toxicities of nanoscale titanium dioxide particles in the roots and leaves of wheat seedlings. RSC Adv 9:19243–19252. https://doi.org/10.1039/c9ra02984b

Chutipaijit S, Sutjaritvorakul T (2020) Enhancements of growth and metabolites of indica rice callus (*Oryza sativa* L . cv . pathumthani1) using TiO_2 nanoparticles (NANO-TiO_2). Dig J Nanomater biostructures 15: 483–489 https://chalcogen.ro/483_ChutipaijiTS.pdf

Crabtree RH (2000) A new type of hydrogen bond. Science 282:2000–2001. https://doi.org/10.1126/science.282.5396.2000

Dai Y, Wang Z, Zhao J, Xu L, Xu L, Yu X, Wei Y, Xing B (2018) Interaction of CuO nanoparticles with plant cells: internalization, oxidative stress, electron transport chain disruption, and toxicogenomic responses. Environ Sci Nano 5:2269–2281. https://doi.org/10.1039/C8EN00222C

Deng X, Cheng J, Hu X, Wang L, Li D, Gao K (2017) Biological effects of TiO_2 and CeO_2 nanoparticles on the growth , photosynthetic activity , and cellular components of a marine diatom *Phaeodactylum tricornutum*. Sci Total Environ 575:87–96. https://doi.org/10.1016/j.scitotenv.2016.10.003

Faisal M, Saquib Q, Alatar AA, Khedhairy AA, Ahmed M, Ansari SM, Alwathnani HA, Dwivedi S, Musarrat J, Praveen S (2016) Cobalt oxide nanoparticles aggravate DNA damage and cell death in eggplant via mitochondrial swelling and NO signaling pathway. Biol Res 49:1–13. https://doi.org/10.1186/s40659-016-0080-9

Fielding JL, Hall JL (1978) A biolchemical and cytochemical study of peroxidase activity in roots of *pisum sativum*: I. a comparison of dab-peroxidase and guaiacol-peroxidase with particular emphasis on the properties of cell wall activity. J Exp Bo 29:969–981. https://doi.org/10.1016/j.desal.2010.10.052

Frohlich E (2013) Cellular targets and mechanisms in the cytotoxic action of non-biodegradable engineered nanoparticles. Curr Drug Metab 14:976–988. https://doi.org/10.1016/bs.coac.2018.10.001

Ghoto K, Simon M, Gao G, Li P (2020) Physiological and root exudation response of maize seedlings to TiO_2 and SiO_2 nanoparticles exposure. Bionanoscience 10:473–485. https://doi.org/10.1007/s12668-020-00724-2

Gould KS, Markham KR, Smith RH, Goris JJ (2000) Functional role of anthocyanins in the leaves of *Quintinia serrata* a. Cunn J Exp Bot 51:1107–1115. https://doi.org/10.1093/jexbot/51.347.1107

Haider AJ, Jameel zainab N, Al-hussaini IHM (2019) Review on : titanium dioxide applications. Energy Procedia 157:17–29. https://doi.org/10.1016/j.egypro.2018.11.159

Hernández JA, Almansa MS (2002) Short-term effects of salt stress on antioxidant systems and leaf water relations of pea leaves. Physiol Plant 115:251–257. https://doi.org/10.1034/j.1399-3054.2002.1150211.x

Hernandez-Viezcas JA, Castillo-Michel H, Peralta-Videa JR, Gardea-Torresdey JL (2015) Interactions between CeO_2 nanoparticles and the desert plant Mesquite: a spectroscopy approach. Sustain Chem Eng 4:1187–1192. https://doi.org/10.1021/acssuschemeng.5b01251

Hong F, Yang F, Liu C, Gao Q, Wan Z, Gu F, Wu C, Ma Z, Zhou J, Yang P (2005a) Influences of nano-TiO_2 on the chloroplast aging of spinach under light. Biol Trace Elem Res 104:249–260. https://doi.org/10.1385/BTER:104:3:249

Hong F, Zhou J, Liu C, Yang F, Wu C, Zheng L, Yang P (2005b) Effect of nano-TiO_2 on photochemical reaction of chloroplasts of spinach. Biol Trace Elem Res 105:269–279. https://doi.org/10.1385/BTER:105:1-3:269

Hong SJ, Li YY, Na NR, Su TZ, Zhi L, Yongwei Z, Hui S, Wei L, Brigitte G (2017) Silver nanoparticles induced reactive oxygen species via photosynthetic energy transport imbalance in an aquatic plant. Nanotoxicology 11:157–167. https://doi.org/10.1080/17435390.2017.1278802

Hund-rinke K, Sinram T, Schlich K, Nickel C, Dickehut HP, Schmidt M, Kühnel D (2020) Attachment efficiency of Nanomaterials to algae as an important criterion for Ecotoxicity and grouping. Nanomaterials 10:1–18. https://doi.org/10.3390/nano10061021

Hussain S, Iqbal N, Brestic M, Ahmed S, Wen B, Gao Y, Liu W, Yang W (2019) Changes in morphology, chlorophyll fluorescence performance and rubisco activity of soybean in response to foliar application of ionic titanium under normal light and shade environment. Sci Total Environ 658:626–637. https://doi.org/10.1016/j.scitotenv.2018.12.182

Ishida A, Ookubo K, Ono K (1987) Formation of hydrogen peroxide by NAD (P) H oxidation with isolated cell wall-associated peroxidase from cultured liverwort cells. Plant Cell Physiol 28:723–726. https://doi.org/10.1093/oxfordjournals.pcp.a077349

Jaberzadeh A, Moaveni P, Tohidi Moghadam HR, Zahedi H (2013) Influence of bulk and nanoparticles titanium foliar application on some agronomic traits, seed gluten and starch contents of wheat subjected to water deficit stress. Not Bot Horti Agrobot Cluj-Napoca 41:201–207. https://doi.org/10.15835/NBHA4119093

Jahan S, Alias YB, Bakar AF, YusoffI (2018) Toxicity evaluation of ZnO and TiO_2 nanomaterials in hydroponic red bean (*Vigna angularis*) plant: physiology, biochemistry and kinetic transport. J Environ Sci 72:1–13. https://doi.org/10.1016/j.jes.2017.12.022

Janků M, Tichá T, Luhová L, Petřivalský M (2019) Compartmentalization of reactive oxygen species and nitric oxide production in plant cells. In: Reactive oxygen, nitrogen and sulfur species in plants:production, Metabolism, Signaling and Defense Mechanisms, pp 923–945. https://doi.org/10.1002/9781119468677.ch40

Juárez-Maldonado A, Ortega-ort H, Morales-Díaz AB, González-Morales S, Morelos-Moreno Á, Cabrera-De la Fuente M, Sandoval-Rangel A, Cadenas-Pliego G, Benavides-Mendoza A (2019) Nanoparticles and nanomaterials as plant biostimulants. Int J Mol Sci Hypothesis 20:1–19. https://doi.org/10.3390/ijms20010162

Khatri K, Rathore MS (2018) Plant nanobionics and its applications for developing plants with improved photosynthetic capacity. In: Photosynthesis - From its Evolution to Future Improvements in Photosynthetic Efficiency Using Nanomaterials. https://doi.org/10.5772/intechopen.76815

Klug HP, Alexande LE (1974) X-ray diffractions procedures for polycrystalline and Anwrphous materials. 2rd edn. Wiley, New York 79:553–553. https://doi.org/10.1002/bbpc.19750790622

Lammers K, Arbuckle-keil G, Dighton J (2009) FT-IR study of the changes in carbohydrate chemistry of three New Jersey pine barrens leaf litters during simulated control burning. Soil Biol Biochem 41:340–347. https://doi.org/10.1016/j.soilbio.2008.11.005

Lead JR, Batley GE, Alvarez PJJ, Croteau M, Richard D, Mclaughlin MJ, Judy JD, Schirmer K (2018) Nanomaterials in the environment: behavior, fate, bioavailability, and effects—an updated review. Environ Toxicol Chem 37:2029–2063. https://doi.org/10.1002/etc.4147

Lei Z, Mingyu S, Xiao W, Chao L, Chunxiang Q, Liang C, Hao H, Xiaoqing L, Fashui H (2008) Antioxidant stress is promoted by nano-anatase in spinach chloroplasts under UV-B radiation. Biol Trace Elem Res 121:69–79. https://doi.org/10.1007/s12011-007-8028-0

Lichtenthaler HK, Wellburn AR (1983) Determinations of total carotenoids and chlorophylls a and b of leaf extracts in different solvents. Biochemical Society transactions. Water Sci Technol 11:591–592. https://doi.org/10.2166/wst.2006.891

Ma C, Chhikara S, Xing B, Musante C, White JC, Dhankher OP (2013) Physiological and molecular response of *Arabidopsis thaliana* (L.) to nanoparticle cerium and indium oxide exposure. ACS Sust Chem Eng 1:768–778. https://doi.org/10.1021/sc400098h

Middepogu A, Hou J, Gao X, Lin D (2018) Effect and mechanism of TiO_2 nanoparticles on the photosynthesis of *Chlorella pyrenoidosa*. Ecotoxicol Environ Saf 161:497–506. https://doi.org/10.1016/j.ecoenv.2018.06.027

Missaoui T, Smiri M, Chemingui H, Alhalili Z, Hafiane A (2020) Disturbance in mineral nutrition of fenugreek grown in water polluted with nanosized titanium dioxide. Bull Environ Contam Toxicol In Press 106:327–333. https://doi.org/10.1007/s00128-020-03051-0

Missaoui T, Smiri M, Chemingui H, Jbira E, Hafiane A (2018) Regulation of mitochondrial and cytosol antioxidant systems of fenugreek (*Trigonella foenum graecum* L.) exposed to Nanosized titanium dioxide. Bull Environ Contam Toxicol 101:326–337. https://doi.org/10.1007/s00128-018-2414-5

Missaoui T, Smiri M, Chmingui H, Hafiane A (2017) Effects of nanosized titanium dioxide on the photosynthetic metabolism of fenugreek (*Trigonella foenum-graecum* L .). C R Biol 340:499–511. https://doi.org/10.1016/j.crvi.2017.09.004

Morales MI, Rico CM, Hernandez-viezcas JA, Nunez JE, Barrios AC, Tafoya A, Flores-marges JP, Peralta-videa JR, Gardea-torresdey JL (2013) Toxicity assessment of cerium oxide nanoparticles in cilantro *(Coriandrum sativum* L.) plants grown in organic soil. J Agric Food Chem 61:6224–6230. https://doi.org/10.1021/jf401628v

Morteza E, Moaveni P, Farahani HA, Kiyani M (2013) Study of photosynthetic pigments changes of maize (*Zea mays* L.) under nano TiO_2 spraying at various growth stages. Springerplus 2:1–5. https://doi.org/10.1186/2193-1801-2-247

Naghdi M, Metahni S, Ouarda Y, Brar SK (2017) Instrumental approach toward understanding nano-pollutants. Nanotechnol Environ Eng 2:1–17. https://doi.org/10.1007/s41204-017-0015-x

Nakano Y, Asada K (1981) Hydrogen peroxide is scavenged by ascorbate-specific peroxidase in spinach chloroplasts. Plant Cell Physiol 22:867–880. https://doi.org/10.1093/oxfordjournals.pcp.a076232

Naumann D, Helm D, Labischinski H, Giesbrecht P (1991) The characterisation of microorganisms by Fourier-transform infrared spectroscopy (FT-IR). In: Nelson WH (ed) Modern techniques for rapid microbiological analysis. VCH Publ, New York, pp 43–96. https://doi.org/10.1371/journal.pone.0097881

Nile SH, Baskar V, Selvaraj D, Nile A (2020) Nanotechnologies in food science: applications, recent trends, and future perspectives. Nano-Micro Lett 12:1–34. https://doi.org/10.1007/s40820-020-0383-9

Niltharach A, Kityakarn S, Worayingyong A, Thienprasert JT, Klysubune W, Songsiriritthigulef P, Limpijumnong S (2012) Structural characterizations of sol – gel synthesized TiO_2 and Ce/TiO_2 nanostructures. Phys B 407:2915–2918. https://doi.org/10.1016/j.physb.2011.08.108

Ogunkunle CO, Adegboye EF, Okoro HK, Vishwakarma V, Alagarsamy K, Fatoba PO (2020) Effect of nanosized anatase TiO_2 on germination, stress defense enzymes, and fruit nutritional quality of *Abelmoschus esculentus* (L .) *Moench* (okra). Arab J Geosc 13:1–13. https://doi.org/10.1007/s12517-020-5121-6

Piro G, Leucci MR, Waldron K, Dalessandro G (2003) Exposure to water stress causes changes in the biosynthesis of cell wall polysaccharides in roots of wheat cultivars varying in drought tolerance. Plant Sci 165:559–569. https://doi.org/10.1016/S0168-9452(03)00215-2

Planchuelo G, Von Der Lippe M, Kowarik I (2019) Landscape and urban planning untangling the role of urban ecosystems as habitats for endangered plant species. Landsc Urban Plan 189:320–334. https://doi.org/10.1016/j.landurbplan.2019.05.007

Rico C, Hong J, Morales MI, Zhao L, Barrios AC, Zhang Y, Peralta-videa JR, Gardea-torresdey JL (2013) Effect of cerium oxide nanoparticles on rice : a study involving the antioxidant defense system and in vivo fluorescence imaging. Environ Sci Technol 47:5635–5642. https://doi.org/10.1021/es401032m

Satalkar P, Elger BS, Shaw DM (2016) Defining nano, nanotechnology and nanomedicine: why should it matter? Sci Eng Ethics 22:1255–1276. https://doi.org/10.1007/s11948-015-9705-6

Scott M (2014) Sunscreen compositions for application to plants. United States patent US 8,986,741B2.https://patentimages.storage.googleapis.com/b7/30/87/0b441978552acf/US8986741.pdf

Shabbir A, Khan MMA, Ahmad B, Sadiq Y, Jaleel H, Uddin M (2019) Efficacy of TiO_2 nanoparticles in enhancing the photosynthesis, essential oil and khusimol biosynthesis in *Vetiveria zizanioides* L . Nash. Photosynthetica 57:599–606. https://doi.org/10.32615/ps.2019.071

Shang Y, Wu F, Wei S, Guo W, Chen J, Huang W, Hu M, Wang Y (2020) Specific dynamic action of mussels exposed to TiO2 nanoparticles and seawater acidification. Chemosphere 241:125104. https://doi.org/10.1016/j.chemosphere.2019.125104

Siddiqui MH, Al-Whaibi MH, Firoz M, Al-Khaishany MY (2015) Nanotechnology and plant sciences. Springer International Publishing, Switzerland, p 305. https://doi.org/10.1007/978-3-319-14502-0

Silva S, Craveiro SC, Oliveira H, Calado AJ, Ricardo JB, Silva AMS, Santos C (2017) Wheat chronic exposure to TiO_2-nanoparticles: Cyto- and genotoxic approach. Plant Physiol Biochem 121:89–98. https://doi.org/10.1016/j.plaphy.2017.10.013

Silva S, Miguel J, De Oliveira PF, Celeste M, Silva AMS (2019) Antioxidant mechanisms to counteract TiO_2 - nanoparticles toxicity in wheat leaves and roots are organ dependent. J Hazard Mater 380:1–10. https://doi.org/10.1016/j.jhazmat.2019.120889

Singleton VL, Rossi JAJ (1965) Colorimetry of total phenolics with phosphomolybdic- phosphotungstic acid reagents. Am J Enol Vitic 16:144–158. https://doi.org/10.1017/CBO9781107415324.004

Smiri M, Chaoui A, El Ferjani E (2009) Respiratory metabolism in the embryonic axis of germinating pea seed exposed to cadmium. J Plant Physiol 166:259–269. https://doi.org/10.1016/j.jplph.2008.05.006

Song C, Huang M, White JC, Zhang X, Wang W, Kyei Sarpong C, Hussain Z, Zhang H, Zhao L, Wang Y (2020) Metabolic profile and physiological response of cucumber foliar exposed to engineered MOS_2 and TiO_2 nanoparticles. NanoImpact 20:1–10. https://doi.org/10.1016/j.impact.2020.100271

Tighe-neira R, Reyes-díaz M, Nunes-nesi A, Recio G, Carmona E, Corgne A, Rengel Z, Inostroza-blancheteau C (2020) Titanium dioxide nanoparticles provoke transient increase in photosynthetic performance and differential response in antioxidant system in *Raphanus*. Sci Hortic (Amsterdam) 269:1–10. https://doi.org/10.1016/j.scienta.2020.109418

Tripathi DK, Singh S, Singh S, Pandey R, Pratap V, Sharma NC, Mohan S, Kishore N, Kumar D (2017) Plant physiology and biochemistry an overview on manufactured nanoparticles in plants : uptake, translocation, accumulation and phytotoxicity. Plant Physiol Biochem 110:2–12. https://doi.org/10.1016/j.plaphy.2016.07.030

Verma G, Srivastava D, Tiwari P, Chakrabarty D (2019) ROS modulation in crop plants under drought stress. In: reactive oxygen, nitrogen and sulfur species in plants: production, metabolism, signaling and defense mechanisms. John Wiley & Sons Ltd, West Sussex, UK, pp 311–336. https://doi.org/10.1002/9781119468677.ch13

Vittori Antisari L, Carbone S, Gatti A, Vianello G, Nannipieri P (2014) Uptake and translocation of metals and nutrients in tomato grown in soil polluted with metal oxide (CeO_2, Fe_3O_4, SnO_2, TiO_2) or metallic (Ag, co, Ni) engineered nanoparticles. Environ Sci Pollut Res 22:1841–1853. https://doi.org/10.1007/s11356-014-3509-0

Wang L, Sun J, Lin L, Funa Y, Aleniusc H, Lindseyd K, Chen C (2020) Silver nanoparticles regulate Arabidopsis root growth by concentration-dependent modification of reactive oxygen species accumulation and cell division. Ecotoxicol Environ Saf 190:1–9. https://doi.org/10.1016/j.ecoenv.2019.110072

Wu B, Zhu L, Le XC (2017) Metabolomics analysis of TiO_2 nanoparticles induced toxicological effects on rice (*Oryza sativa* L.). Environ Pollut 230:302–310. https://doi.org/10.1016/j.envpol.2017.06.062

Xia B, Chen B, Sun X, Qu K, Ma F, Du M (2015) Interaction of TiO_2 nanoparticles with the marine microalga N*itzschia closterium*: growth inhibition, oxidative stress and internalization. Sci Total Environ 508:525–533. https://doi.org/10.1016/j.scitotenv.2014.11.066

Yang F, Hong F, You W, Liu C, Gao F, Wu C, Yang P (2006) Influences of nano-anatase TiO_2 on the nitrogen metabolism of growing spinach. Biol Trace Elem Res 110:179–190. https://doi.org/10.1385/BTER:110:2:179

Zayneb C, Bassem K, Zeineb K, Grubb CD, Noureddine D, Hafedh M (2015) Physiological responses of fenugreek seedlings and plants treated with cadmium. Environ Sci Pollut Res 22:10679–10689. https://doi.org/10.1007/s11356-015-4270-8

Zhishen J, Mengcheng TJW, Jianming W (1999) The determination of flavonoid contents in mulberry and their scavenging effects on superoxide radicals. Food Chem 64(4):555–559. https://doi.org/10.1016/S0308-8146(98)00102-2

Zuverza-mena N, Armendariz R, Peralta-videa JR (2016) Effects of silver nanoparticles on radish sprouts : root growth reduction and modifications in the nutritional value. Front Plant Sci 7:1–11. https://doi.org/10.3389/fpls.2016.00090

Affiliations

Takwa Missaoui[1,2] · Moêz Smiri[1,3] · Hajer Chemingui[1] · Amor Hafiane[1]

[1] Laboratory of Water, Membranes and Environment Biotechnology (LEMBE), Technopole of Borj Cedria (CERTE), 2050 Hammam-Lif, Tunisia

[2] National Agronomy Institute of Tunis, 43 Avenue Charles Nicolle, 1082 Tunis, Tunisia

[3] College of Sciences and Arts – Sajer, Shaqra University, Riyadh, Saudi Arabia